

Studying the Higgs Potential at the e^+e^- Linear Collider

Marco Battaglia*

CERN, CH-1211 Geneva 23, Switzerland

Eduard Boos†

Institute of Nuclear Physics, Moscow State University, 119899 Moscow, Russia

Weiming Yao‡

LBNL, Berkeley CA 94720, USA

(Dated: October 15, 2001)

The determination of the shape of the Higgs potential is needed to complete the investigation of the Higgs profile and to obtain a direct experimental proof of the mechanism of electro-weak symmetry breaking. This can be achieved, at a linear collider, by determining the Higgs triple self-coupling g_{HHH} in the processes $e^+e^- \rightarrow H^0H^0Z^0$ and $H^0H^0\nu_e\bar{\nu}_e$ and, possibly, the quartic coupling. This paper summarises the results of a study of the expected accuracies on the determination of g_{HHH} at a TeV-class LC and at a multi-TeV LC. The statistical dilution arising from contributions not sensitive to the triple Higgs vertex, can be reduced by means of variables sensitive to the kinematics and the spin properties of the reactions.

I. INTRODUCTION

The detailed study of the Higgs potential represents a conclusive test of the mechanism of symmetry breaking and mass generation. After the discovery of an elementary Higgs boson and the test of its couplings to quarks, leptons and gauge bosons, a further proof of the Higgs mechanism will be the experimental evidence that the Higgs field potential has the properties required for breaking the electro-weak symmetry. In the Standard Model (SM), the Higgs potential can be written as $V(\Phi^*\Phi) = \lambda(\Phi^*\Phi - \frac{1}{2}v^2)^2$. A probe of the shape of this potential comes from the determination of the triple and quartic Higgs self-couplings [1, 2, 3, 4]. The triple coupling can be expressed, in the SM, as $g_{HHH} = \frac{3}{2} \frac{M_H^2}{v}$ where $v=246$ GeV and M_H can be determined to $\mathcal{O}(100)$ MeV accuracy. An accurate test of this relation may reveal the extended nature of the Higgs sector. This can be achieved by observing the deviations, arising in a generic 2HDM or in a SUSY scenario, from the SM prediction above. Accurate data can be analysed in terms of an effective Lagrangian to establish the relationships between the Higgs self-couplings and the size of anomalous terms of other nature.

This paper summarises the findings of a comparative study of the potential of a TeV-class e^+e^- linear collider (LC) and of a second-generation multi-TeV LC in the study of the Higgs potential through the analysis of the $e^+e^- \rightarrow H^0H^0Z^0$ and $H^0H^0\nu_e\bar{\nu}_e$ processes in SM. The opportunity, offered by a LC, to study the Higgs potential may be unique, as no evidence that the SM triple Higgs vertex is experimentally accessible at hadron colliders has been obtained so far [5].

At the linear collider the triple Higgs coupling g_{HHH} can be accessed by studying multiple Higgs production in the processes $e^+e^- \rightarrow H^0H^0Z^0$ and $H^0H^0\nu_e\bar{\nu}_e$ that are sensitive to the triple Higgs vertex. The first process is more important at lower values of the centre-of-mass energy, \sqrt{s} , and for Higgs boson masses in the range $115 \text{ GeV} < M_H < 130 \text{ GeV}$, with a cross section of the order of 0.15 fb for $M_H = 120 \text{ GeV}$. The second process becomes sizeable at collision energies above 1 TeV and ensures sensitivity to the triple Higgs vertex for heavier Higgs masses. It also provides a cross section larger by a factor $\simeq 7$. The quartic Higgs coupling remains elusive. The cross sections for the $HHHZ$ and $HHH\nu\bar{\nu}$ processes are reduced by three order of magnitude compared to those for the double Higgs production. In the most favourable configuration, a 10 TeV e^+e^- collider operating with a luminosity of $10^{35} \text{ cm}^{-2} \text{ s}^{-1}$ would be able to produce only about five such events in one year ($=10^7 \text{ s}$) of operation for $M_H = 120 \text{ GeV}$ (see Table I).

A $\gamma\gamma$ collider has also access to the triple Higgs couplings through the processes $\gamma\gamma \rightarrow HH$ and $\gamma\gamma \rightarrow HHW^+W^-$. However the cross section of the first process is suppressed by the effective $H\gamma\gamma$ coupling, compared to e^+e^- collisions, and that of the second is only 0.35 fb at $\sqrt{s_{ee}} = 1 \text{ TeV}$ for $M_H = 120 \text{ GeV}$. A muon collider

*Marco.Battaglia@cern.ch

†boos@theory.sinp.msu.ru

‡wmiao@lbl.gov

does not offer significant advantages, compared to a high energy e^+e^- LC. The most favourable production cross sections are comparable: the $\mu^+\mu^- \rightarrow HH\nu_\mu\bar{\nu}_\mu$ process has $\sigma=0.8$ fb-2.7 fb for $\sqrt{s} = 3$ TeV-7 TeV. On the contrary, the $\mu^+\mu^- \rightarrow HH$ reaction, which would be unique to a muon collider, is strongly suppressed.

A major problem arising in the extraction of g_{HHH} from the measurement of the double Higgs production cross section comes from the existence of diagrams that lead to the same final states but do not include a triple Higgs vertex. The resulting dilution $\frac{\delta g_{HHH}/g_{HHH}^{SM}}{\delta\sigma/\sigma^{SM}}$, is significant for all the processes considered. It is therefore interesting to explore means to enhance the experimental sensitivity to the signal diagrams with additional variables. In this study the H decay angle in the HH rest frame and the HH invariant mass have been considered.

The cross section computation and the event generation at parton level have been performed using the COMPHEP [6] program where the g_{HHH} coupling and the M_H mass have been varied. Partons have been subsequently fragmented according to the parton shower model using PYTHIA 6 [7]. The resulting final state particles, for the $HH\nu\bar{\nu}$ channel, have been processed through the SIMDET [8] parametrised detector simulation and the reconstruction analysis performed. Background processes for the $HH\nu\bar{\nu}$ channel have also been simulated and accounted in the analysis. The centre-of-mass energies of 0.5 TeV / 0.8 TeV and 3 TeV, representative of the anticipated parameters for a TeV-class LC, such as TESLA or a X-band collider, and a multi-TeV collider, such as CLIC, have been chosen with an integrated luminosity of 1 ab^{-1} and 5 ab^{-1} respectively. In this study, unpolarised beams are assumed. Polarizing the beams brings a gain of a factor of two for the HHZ cross section and of four for $HH\nu\bar{\nu}$.

II. THE HHZ PROCESS

The g_{HHH} determination from the measurement of the $e^+e^- \rightarrow HHZ$ cross-section has been already extensively discussed in its theoretical [3] and experimental issues [9]. A e^+e^- collider operating at $\sqrt{s} = 500$ GeV can measure the HHZ production cross section to about 15% accuracy if the Higgs boson mass is 120 GeV, corresponding to a fractional accuracy of 23% on g_{HHH} . At higher \sqrt{s} energies the dilution increases and it becomes interesting to combine a discriminating variable. The invariant mass of the HH system provides with a significant discrimination of the $H^* \rightarrow HH$ process from other sources of HHZ production not involving the triple Higgs vertex. In fact, in the first case the distribution is peaked just above the $2M_H$ kinematic threshold and dumped by the virtuality of the H^* boson while the background processes exhibit a flatter behaviour extending up to the upper kinematic limit $\sqrt{s} - M_Z$ (see Figure 1). These characteristics have been tested to discriminate between the signal triple Higgs vertex contribution and the background processes in genuine HHZ final states. As the phase space increases with increasing \sqrt{s} , for a fixed M_H value, this variable is most effective at larger \sqrt{s} values, i.e. as the dilution effect increases. A likelihood fit to the total number of events and to the normalised binned distribution of the M_{HH} distribution has been performed on HHZ events at generator level for $M_H = 120$ GeV and $\sqrt{s} = 500$ GeV and 800 GeV (see Figure 2). Results are given in Table II. Work is in progress for improving the measurement further by including an additional $e^+e^- \rightarrow HHZ$, where $Z \rightarrow \nu\bar{\nu}$ in the final states.

III. THE $HH\nu\bar{\nu}$ PROCESS

The $e^+e^- \rightarrow HH\nu\bar{\nu}$ process exhibits a significant larger cross-section, compared to HHZ , if the collision energy exceeds 1 TeV. In addition, being the interference of the signal triple Higgs vertex and the other diagrams, leading to $HH\nu\bar{\nu}$, destructive, the total cross section decreases with increasing g_{HHH} , contrary to the case of the HHZ channel. This may represent an important cross-check of the Higgs self coupling contribution, in the case any deviations would be observed in the HHZ cross-section. Since the $HH\nu\bar{\nu}$ production is peaked in the forward region, it is important to ensure that an efficient tagging of the $HH \rightarrow b\bar{b}b\bar{b}$, $W^+W^-W^+W^-$ decay can be achieved. Therefore a full reconstruction of $HH\nu\bar{\nu}$ and $ZZ\nu\bar{\nu}$ events has been performed. The $4b + E_{miss}$ and $4W + E_{miss}$ final states have been considered for the Higgs boson masses of 120 GeV and 180 GeV. The sensitivity to the triple Higgs vertex has been enhanced by studying the angle θ^* made by the H boson, boosted back in the HH rest frame, with the HH direction. Due to the Higgs boson scalar nature, the $\cos\theta^*$ distribution is flat for the signal $H^* \rightarrow HH$ process, while it has been found to be forward and backward peaked for the $HH\nu\bar{\nu}$ contributions from other diagrams [1]. This characteristics is preserved after event reconstruction (see Figure 3) and a fit including the measured cross section and the normalised shape of the $|\cos\theta^*|$ distribution has been performed, similarly to the case of the HHZ channel (see Figure 4). Results are given in Table III. Beam polarisation has not been taken into account. This may provide the ultimate means for pushing the accuracy on g_{HHH} below 5%.

TABLE I: Production cross sections for $e^+e^- \rightarrow HHH\nu\bar{\nu}$

\sqrt{s}	$g_{HHHH}/g_{HHHH}^{SM} = 0.9$	$g_{HHHH}/g_{HHHH}^{SM} = 1.0$	$g_{HHHH}/g_{HHHH}^{SM} = 1.1$
3 TeV	0.400	0.390	0.383
5 TeV	1.385	1.357	1.321
10 TeV	4.999	4.972	4.970

TABLE II: Summary of relative accuracies $\delta g_{HHH}/g_{HHH}$ for $M_H = 120$ GeV and $\int L = 1 \text{ ab}^{-1}$ with the HHZ channel.

\sqrt{s} (TeV)	σ_{HHZ} Only	M_{HH} Fit
0.5	± 0.23 (stat)	± 0.20 (stat)
0.8	± 0.35 (stat)	± 0.29 (stat)

IV. CONCLUSIONS

The study of the triple Higgs couplings will provide a crucial test of the Higgs mechanism of electro-weak symmetry breaking, by directly accessing the shape of the Higgs field potential. e^+e^- linear colliders, where the study of the $e^+e^- \rightarrow HHZ$ and $HH\nu\bar{\nu}$ can be performed with good accuracy, represent a possibly unique opportunity for performing this study. The study of variables sensitive to the triple Higgs vertex and the availability of high luminosity will allow to test the Higgs potential structure to an accuracy of about 20% at a TeV-class collider and to 8% and better in multi-TeV e^+e^- collisions. The quartic coupling appears to remain inaccessible due to its tiny cross-section and the large dilution effect from background diagrams in $HHH\nu\bar{\nu}$.

ACKNOWLEDGMENTS

This study owes much to several colleagues with whom we had the pleasure to discuss before, during and after the Snowmass workshop. In particular we like to thank F. Boudjema, L. Maiani, M. Muhlleitner, K. Desch and P. Gay for their suggestions. E.B. was supported in part by the CERN-INTAS grant 99-0377 and by the INTAS grant 00-0679.

REFERENCES

- [1] F. Boudjema and E. Chopin, Z. Phys. **C73**, 85 (1996), arXiv:hep-ph/9507396.
- [2] V. A. Ilin, A. E. Pukhov, Y. Kurihara, Y. Shimizu, and T. Kaneko, Phys. Rev. **D54**, 6717 (1996), arXiv:hep-ph/9506326.
- [3] A. Djouadi, W. Kilian, M. Muhlleitner, and P. M. Zerwas, Eur. Phys. J. **C10**, 27 (1999), arXiv:hep-ph/9903229.
- [4] A. Djouadi, W. Kilian, M. Muhlleitner, and P. M. Zerwas (1999), arXiv:hep-ph/0001169.
- [5] R. Lafaye, D. J. Miller, M. Muhlleitner, and S. Moretti (2000), hep-ph/0002238.
- [6] A. Pukhov et al. (1999), arXiv:hep-ph/9908288.
- [7] T. Sjostrand, L. Lonnblad, and S. Mrenna (2001), arXiv:hep-ph/0108264.
- [8] M. Pohl and H. J. Schreiber, *Simdet - version 3: A parametric monte carlo for a tesla detector*, DESY-99-030 (1999).
- [9] C. Castanier, P. Gay, P. Lutz, and J. Orloff (2001), arXiv:hep-ex/0101028.

TABLE III: Summary of relative accuracies $\delta g_{HHH}/g_{HHH}$ for $\int L = 5 \text{ ab}^{-1}$ with the $HH\nu\bar{\nu}$ channel at 3 TeV.

M_H (GeV)	$\sigma_{HH\nu\bar{\nu}}$ Only	$ \cos \theta^* $ Fit
120	± 0.094 (stat)	± 0.070 (stat)
180	± 0.140 (stat)	± 0.080 (stat)

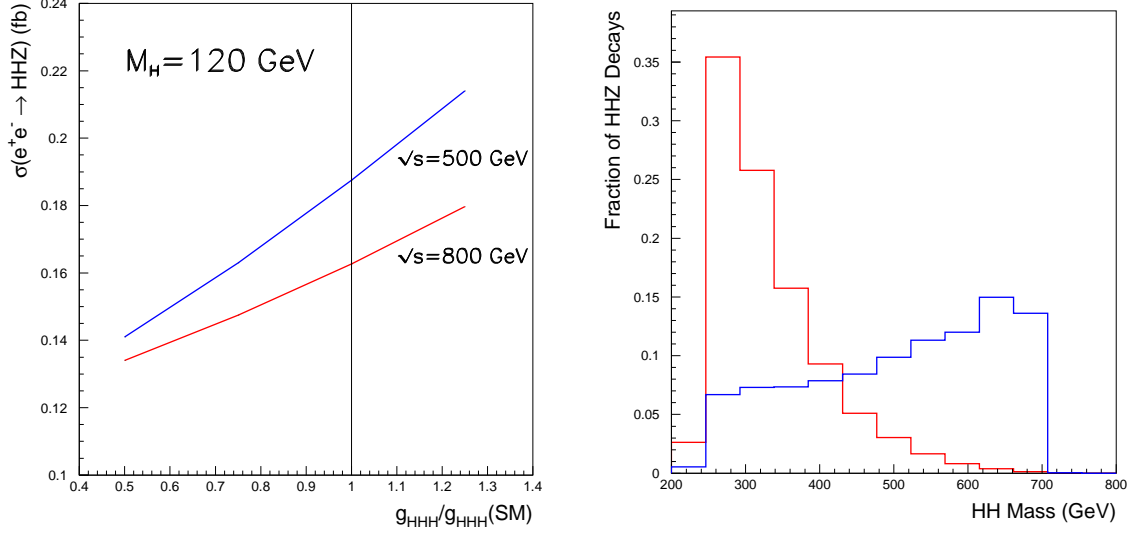


FIG. 1: Left: the dependence of the HHZ cross section on the triple Higgs coupling, normalised to its SM value, for $M_H = 120$ GeV and two \sqrt{s} values. Right: The distribution of the HH invariant mass in HHZ events originating from diagrams containing the triple Higgs vertex (light grey) and other diagrams (dark grey).

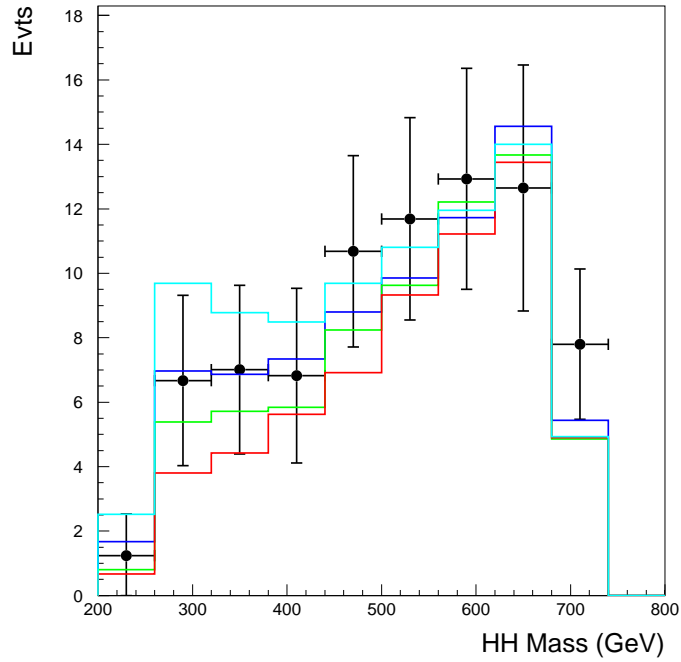


FIG. 2: The generated HH invariant mass distribution for HHZ events obtained for $g_{HHH}/g_{HHH}^{SM} = 1.25, 1.0, 0.75$ and 0.5 with the points with error bars showing the expectation for 1 ab^{-1} of SM data at $\sqrt{s}=0.8$ TeV.

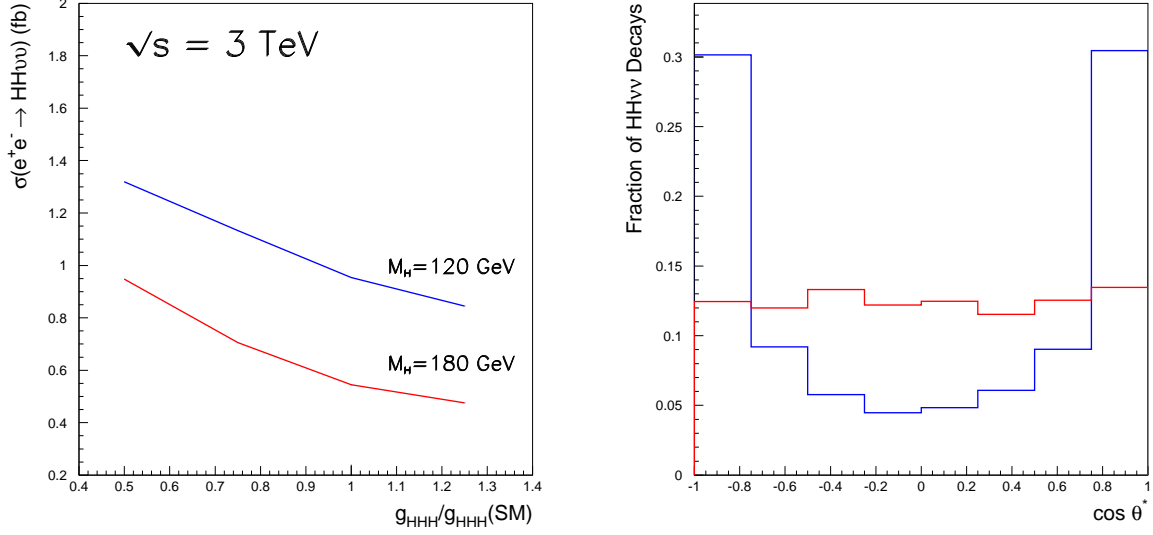


FIG. 3: Left: the dependence of the $HH\nu\bar{\nu}$ cross section on the triple Higgs coupling, normalised to its SM value, for $\sqrt{s} = 3$ TeV and two M_H values. Right: The $\cos \theta^*$ distribution in $HH\nu\bar{\nu}$ events originating from diagrams containing the triple Higgs vertex (light grey) and other diagrams (dark grey).

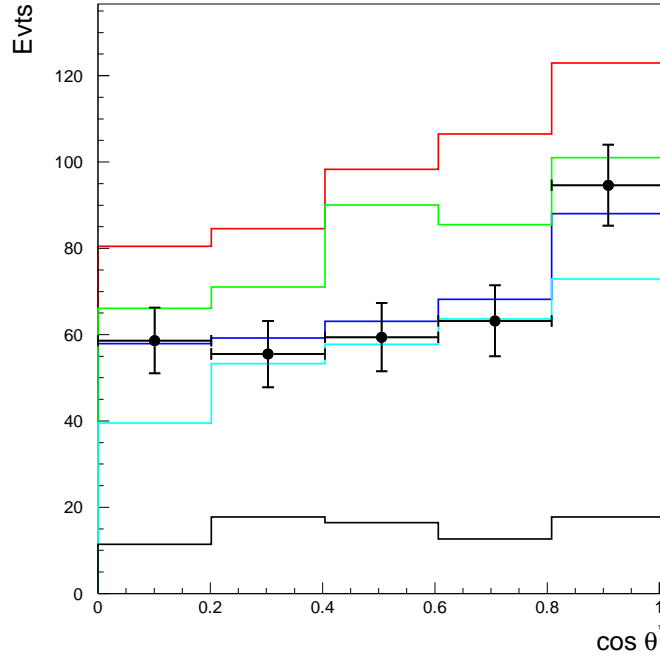


FIG. 4: The reconstructed $|\cos \theta^*|$ distribution for $HH\nu\bar{\nu}$ events obtained for $g_{HHH}/g_{HHH}^{SM} = 1.25, 1.0, 0.75$ and 0.5 with the points with error bars showing the expectation for 5 ab^{-1} of SM data at $\sqrt{s} = 3.0$ TeV.